DOI: 10.21062/mft.2025.073 http://www.journalmt.com

Evaluation of Dimensional Accuracy and Surface Topography of Plastic Parts

Eva Jurickova (0000-0002-8018-7391)[1]*, Stepan Kolomy (0000-0003-3781-692X)[2], Josef Sedlak (0000-0002-9819-8259)[1], Denisa Hrusecka (0000-0003-1459-0040)[1], Petra Sliwkova (0000-0003-4121-2168)[2], Jiri Vitek (0009-0001-2138-6841)[3]
[1]Tomas Bata University in Zlín, Faculty of Management and Economics, Department of Industrial Engineering and Information Systems, Mostní 5139, Zlín 760 01, Czech Republic
[2]Institute of Manufacturing Technology, Faculty of Mechanical Engineering, Brno University of Technology, Czech Republic
[3]Department of Machining, Assembly and Engineering Metrology, Faculty of Mechanical Engineering, Technical University of Ostrava, Czech Republic
*E-mail: jurickova@utb.cz

The objective of this paper is the evaluation of dimensional and geometric accuracy and surface topography of milled parts from plastic. This evaluation was done on 10 samples from various thermoplastics made by extrusion and FDM 3D printing. The samples were then milled. One side was milled dry while the other was milled with cutting fluid, which has improved the texture of the resulting machined surfaces in most cases, for example with printed PLA, where Ra was reduced by 1.8 μm. For determining the dimensional and geometric accuracy, two parameters were chosen, those being distance and parallelism. For evaluating the surface topography, 4 parameters were measured using 2D profile roughness and 3D surface texture. The surface of the prints was greatly improved by machining. The paper ends with practical recommendations for choosing different plastic materials for applications, requiring high dimensional accuracy and low surface roughness.

Keywords: Extrusion, Machining, Plastic, Dimension, 3D printing.

1 Introduction

3D printing is becoming an increasingly popular way of producing plastic parts for both single piece and small batch production. It is a method of additive manufacturing, meaning that material is added to the workpiece to achieve the final shape [1]. This contrasts with machining, where material is removed from an oversized blank [2]. There are multiple methods of 3D printing, that are often divided by the state of the input material into liquid-based, powder-based and solid-based [3; 4; 5]. The most common liquid-based 3D printing process is stereolithography or SLA. With this process, the print bed is submerged in resin, which gets selectively cured by a precise UV scanning laser. The main benefits of SLA printed parts are their smooth surface and isotropic mechanical properties [6; 7]. In powder-based processes, the fine layers of powder are either bonded by a liquid adhesive or are sintered or melted together by a laser [6; 8]. By far the most common process, especially with hobbyists, is fused deposition modelling (FDM). This process works by melting a plastic fibre, called filament, into thin layers [7; 9].

When it comes to 3D printed materials, their mechanical properties are usually worse than those made by injection molding, as shown by Lay et al. [10]. Of note is the finding, that parts made by FDM printing demonstrated higher crystallinity and higher water absorption. Another challenge of FDM prints is their anisotropy, causing mechanical properties to vary in vertical and horizontal orientation. Chacón et al. [11] thus suggest printing in the horizontal orientation and for upright specimens, recommends thicker layers, as it increased tensile and flexural strength. Isotropy can be also improved by exposing printed products to ionizing radiation to crosslink the polymer chains. This was successfully attempted by Shaffer et al. [12] and also showed an increase in resistance to solvents. It is also important to consider that mechanical properties of 3D printed parts vary significantly due to different print parameters including the color of the material, as demonstrated by Wittbrodt and Pearce [13]. Kuznetsov et al. [14] showed that with PLA, layer height plays the most significant role in the inter-layer cohesion of printed specimens, decreasing cohesion with increasing thickness. It was also shown that increasing the size of the nozzle can help improve cohesion. This was even more evident in thicker layers. İncesu et al. [15] also observed, that flexural strength of PLA can be further increased by raising the printing temperature. Similar results were achieved by Hsueh et al. [16], who also tested specimens made from PETG.

It is noted that while both materials mechanical properties improve by increasing the printing temperature, these two plastics behave differently in reaction to change in printing speed. PLA's mechanical properties improve, while those of PETG tended to degrade. Tests also showed that compressive strength of both materials far exceeded their tensile strength. A comparison between PLA and ABS was performed by Rodríguez-Panes et al. [17]. This study showed that even if both materials react similarly to the changes in printing conditions, PLA tends to be more rigid, while ABS showed more ductility and higher sensitivity to layer orientation in relation to the load direction. Also, ABS showed less variability in the results. It is concluded that PLA demonstrated an extremely strong inter-layer bond, that makes it highly suitable for FDM 3D printing. A similar comparison was made by Vinyas et al. [18], who also tested PLA reinforced with carbon fibres, which increased the specimen's tensile strength. Blending PLA with PETG increased the material's hardness. To determine interlayer cohesion, vertically printed specimens are usually needed, which can be challenging and inefficient to manufacture, Torrado et al. [19] suggest using horizontally printed specimens with transversal filling, which were proven to behave equivalently. Mechanical properties of 3D printed products are also dependent on the internal geometry of the infill. Different infill structures were compared by Agrawal et al. [20], who found that concentric infill pattern proved best in fracture resistance, as this structure interrupts crack propagation. This infill pattern also demonstrated the highest ultimate tensile strength and elongation at break. In general, when machining thermoplastics, Alauddin et al [21] recommends cutting speeds exceed 300 m/min and especially highlights the necessity for a very sharp cutting tool to achieve the best surface. When comparing surface quality of cast and 3D printed polyamide, Tezel [22] recognized, that increasing the feed of the tool improves the quality of the machined surfaces of both cast and 3D printed polyamide material, also, that especially on 3D printed parts, the depth of cut is highly influential. Mehtedi et al. [23] conducted research aimed at optimizing cutting parameters in relation to minimizing surface roughness and burr formation on FDM 3D printed parts from PLA and PETG. Optimal parameters for low surface roughness differed from those required for minimal burr, as this required higher cutting parameters. PLA tended to produce higher burrs, which was attributed to its lower glass transition temperature. Pămărac and Petruse [24] reached similar conclusion from their experiments with milling PLA and PETG recommending lower cutting speed for ABS and faster for PLA to avoid overheating the surface. The quality of the machined surface is also highly dependent on the orientation of the print layers. This was examined by Lalegani Dezaki et al. [25], who tested specimens printed at different angles and their experiments show that for the best surface, the tool should be perpendicular to the print layer. One of the significant risks with machining 3D prints is delamination, which was studied by Çevik [26], who recommends using high infill and layer thickness. Drilling into 3D printed materials is also especially susceptible to delamination, which was confirmed by Shunmugesh et al. [27] in their experiments. It was found that drill bits with smaller tip angles performed better than those with larger tip angles. Martín-Bejár et al. [28] experimented with turning carbon-fibre reinforced PLA and found it a suitable substitute for printing with high vertical resolution. As mentioned by Khairusshima et al. [29], machining fibre reinforced composites adds another challenge in the form of excessive tool wear thanks to the abrasive nature of the fibres.

This paper compares the most commonly used materials for extrusion and 3D printing in terms of their surface parameters after machining on a conventional milling machine. The novelty of this paper lies in the creation of a comprehensive list of materials, in extruded and 3D printed form with machining parameters and resulting surface parameters. Also, a series of recommendations are provided to allow for high quality surface finish and low material distortion.

2 Experimental procedure

For the evaluation, 10 samples from different thermoplastics were made. Half of these were made from an extruded blank while the other half were made by FDM 3D printing. Some materials were used for two specimens, but each of those was made by a different manufacturing process. The tested materials are:

Tab. 1 *Selected materials*

Specimen	Material	Abbreviation
1	Polypropylene	PP
2	Polyamide	PA
3	Polyethylene terephthalate	PET
4	Polyoxymethylene	POM
5	Polyethylene ultra-high-molecular-weight	PE-UHMW
6	Polypropylene	PP (3D)
7	Polyamide	PA (3D)
8	Polyethylene terephthalate glycol	PETG (3D)
9	Polylactic acid	PLA (3D)
10	Acrylonitrile polybutadiene styrene	ABS (3D)

2.1 Specimen manufacturing and measurement

The size of the specimens was determined as 35 x 35 x 6 mm as a compromise between a large enough test surface and reduction of waste. To manufacture these specimens, it is first needed to calculate the allowances for milling:

$$p=\frac{5\cdot L}{100}+2 \text{ (mm)} \quad (1)$$

Where:
p…Machining allowance (mm),
L…Length (mm).

- Allowance for thickness $p=\frac{5\cdot 6}{100}+2=2.3$ mm → chosen 3 mm
- Allowance for length and width $p=\frac{5\cdot 35}{100}+2=3.75$ mm → chosen 5 mm

With allowances added, the final size of the blank is determined as 40 x 40 x 9 mm.

2.2 Manufacturing of specimen blanks

Five different materials were chosen. Thickness of the supplied sheets was between 9 and 12 mm, in order to fit the specimen with all machining allowances. From these sheets, the blanks were cut to the required size on a Bomar STG 220 G gravity bandsaw. For the cutting itself, coolant was applied to prevent overheating and degradation of the material. A total of five different blanks were cut, one from each material.

Tab. 2 *Test specimens; The "(3D)" in abbreviation is to distinguish 3D printed specimens from extruded ones*

Specimen	Material	Abbreviation
1	Polypropylene	PP
2	Polyamide	PA
3	Polyethylene terephthalate	PET
4	Polyoxymethylene	POM
5	Polyethylene ultra-high-molecular-weight	PE-UHMW
6	Polypropylene	PP (3D)
7	Polyamide	PA (3D)
8	Polyethylene terephthalate glycol	PETG (3D)
9	Polylactic acid	PLA (3D)
10	Acrylonitrile polybutadiene styrene	ABS (3D)

For 3D printed specimens, the FDM process was chosen. It is the most commonly used and readily available 3D printing process, as prices of simple FDM printers start as low as 4000 CZK. The specimens were first modeled in SolidWorks CAD software and saved as a STL file. The program for the 3D printer was created using PrusaSlicer, a software by Prusa Research a.s. When the programs were ready, the specimen blanks were printed on the Prusa i3 MK3 printer, made by the aforementioned manufacturer. The used printer was also fitted with an accessory, enabling an automatic selection of up to 5 different filaments. The diameter of the filament used is 1.75 mm and the nozzle diameter is 0.4 mm. It is very important to set the print infill to 100% as the printed material must be void free. Finally, the generated code was transferred to a memory card and uploaded to the printer. After each specimen finished printing, it was gently removed from the bed, which was then clean a prepared for the next part.

2.3 Machining of specimens

After all the blanks were cut from sheets and printed, the next step is machining, in this case milling. For this, a tool has to be chosen. The selected tool was a 12-tooth cylindrical milling cutter from high-speed steel. The wear of the tool was not taken into consideration. The milling machine used in this paper is the TOS FNK 25 A, a light-duty belt-driven gearhead knee mill. Cutting parameters, namely feeds and speeds, were determined according to recommendations of the supplier [30]. The spindle speed was calculated using the following formula and rounded down to the nearest available speed setting of the milling machine:

$$n=\frac{1000\cdot v_c}{\pi\cdot d} \text{ (min}^{-1}\text{)} \quad (2)$$

Where:
n…Spindle speed (min^{-1}),
v_c…Cutting speed (m.min^{-1}),
D…Tool diameter (mm).

First, the sides of the blanks were milled square to ensure they can be securely clamped to the milling machine. Then, the two large surfaces were machined. From each of these, 1.5 mm of material was removed. These surfaces were used for evaluation. On each specimen, one surface was machined with cutting fluid, while the other was cut dry. The sides that were cut with cutting fluid were marked with permanent marker to distinguish them from the dry ones. In total, this created 20 individual surfaces to be measured.

Tab. 3 *Cutting parameters for the individual materials*

Specimen	Material	Cutting speed (m·min^{-1})	Calculated spindle speed (min^{-1})	Depth of cut (mm)	Feed (mm·min-1)
1, 6	PP, PP (3D)	230	915	1.5	315
2, 7	PA, PA (3D)	230	915	1.5	315
3	PET	150	637	1.5	224
4	POM	230	915	1.5	315
5	PE-UHMW	230	915	1.5	315
8	PETG (3D)	150	637	1.5	224
9	PLA (3D)	150	637	1.5	224
10	ABS (3D)	230	915	1.5	315

Fig. 1 *Finished specimens, ready to be measured*

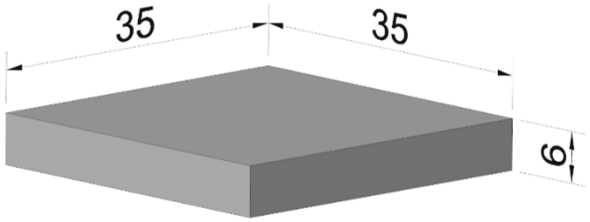

Fig. 2 *Dimensions of finished specimens*

2.4 Measurement

First, the surface quality of the specimens was measured. For the evaluation, the most commonly used parameters of surface topography were used. In 2D, those were:

- Ra – Arithmetic average profile height deviation,
- Rz – Maximum peak to valley height over assessment length.

For 3D, these parameters were:

- Sa – Arithmetic average of absolute values of texture height,
- Sz – Average difference between highest and lowest points.

These values were measured using optical measurement device Talysurf CCI with the included software package TalyMap Platinum. This machine works on the principle of coherence correlation interferometry and offers 0.01 nm of vertical resolution. For this test, a 20x lens was used. The size of the evaluated surface was 0.825 x 0.825 mm and it was sampled at 1024 x 1024 points. The same measurement conditions were used for all specimens and to get relevant results, the measurement was repeated three times for each specimen.

After measuring the surface, the specimens were carefully moved to a Werth ScopeCheck CMM for the measurement of dimensional and geometric accuracy, namely distance between the opposing surfaces, and their parallelism. Before each measurement, the specimen was securely clamped to a small vise. The measurement was realized with a touch probe with a 21 mm long shaft and 3 mm ruby tip. On each surface, a grid of 16 points was created, which were then evaluated.

3 Results and discussion

3.1 Dimensional and geometric accuracy

To obtain more accurate results, three measurements of both distance and parallelism were performed. The results from these measurements were compiled in graph 1, standard deviation being shown in red. The (3D) suffix denotes the specimens made by 3D printing. As seen in the graph, the highest deviation of distance was measured on the PET specimen. This could have been caused by many reasons, most of which include the human factor. Such high deviation with the PET specimen also could have been caused by improper fastening in the vise or impurity on the milling cutter. Although the deviation was high compared to the other specimens, it is important to note that in machining plastics, it is still not extraordinarily large. For example, in the case of steel the lower surface roughness was achieved [31, 32]. Not only in case of the steel machining but also when machining hard to machine material such as UMCo50 Cobalt Superalloy [33].

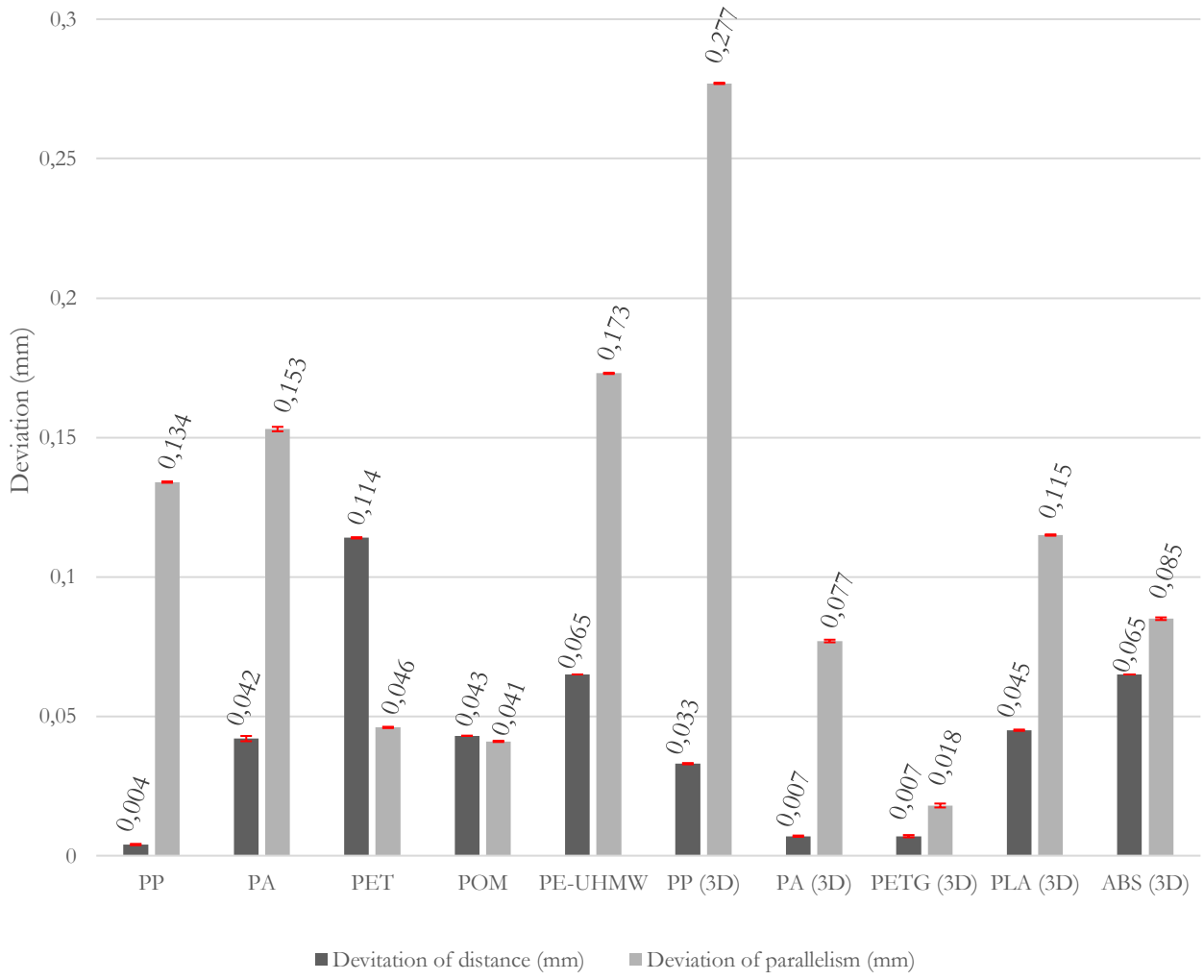

Graph 1 *Deviation from nominal distances and parallelism between evaluated surfaces*

3.2 Surface topography

Of the 10 specimens, each was machined from two opposing sides. One with cutting fluid and one without, resulting in 20 total evaluated surfaces. Due to the large number of resulting values, only some were highlighted. All measured parameters were described in chapter 2.5. Graph 2 shows the resulting values of Ra. It is noticeable that Ra remains consistent between the specimens made by extrusion. Also, the use of cutting fluid improved the quality of the machined surface in 80% of cases. In the graph, suffixes + and – represent, whether cutting fluid was used or not respectively. A disproportional increase in Rz is noted for the 3D printed materials cut with fluid. This is a critical finding, implying that for additively manufactured polymer structures, the use of cutting fluid (as opposed to dry cutting) may be detrimental to the extreme peak-to-valley height, possibly due to chip adhesion or interaction with the material's layered microstructure, again causing high Rz values that are not fully reflected by the Ra metric.

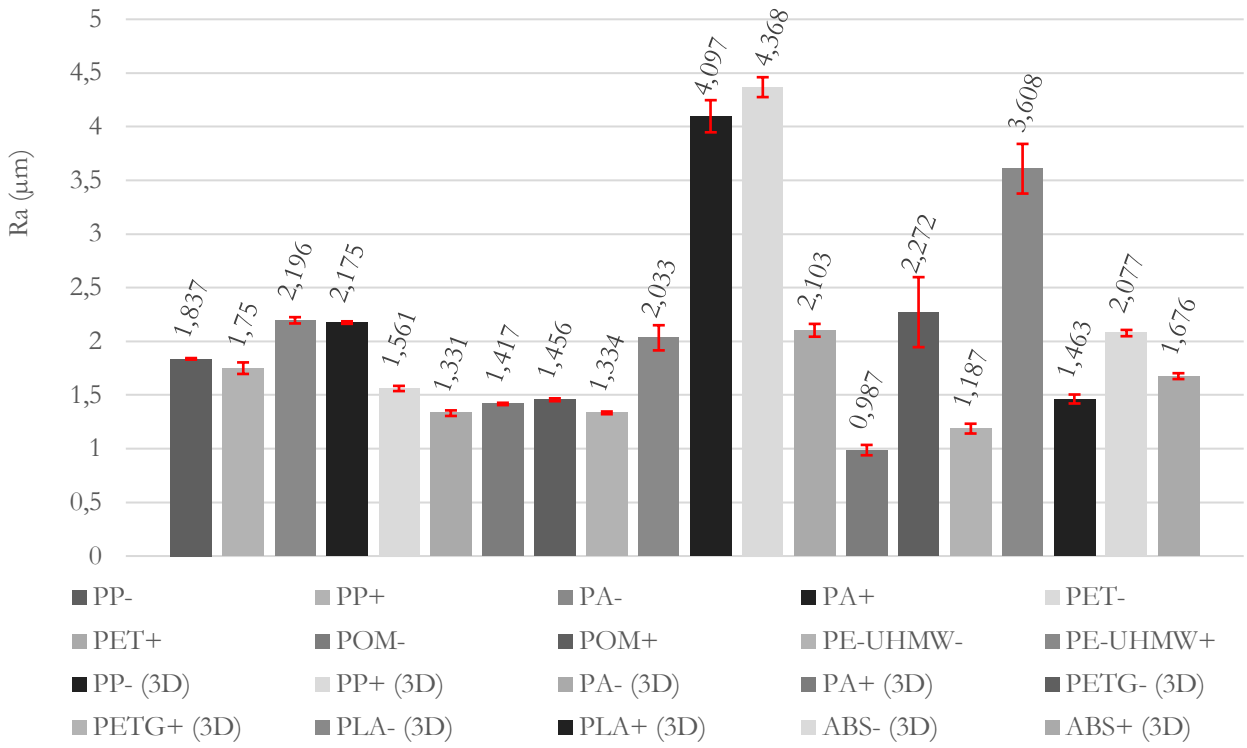

Graph 2 *Arithmetic average surface roughness Ra of evaluated surfaces*

In graph 3 are shown the resulting values of the maximum imperfection height Rz. The measured roughness is similar to the Ra graph with few differences such as the increase in dry cut polyamide (PA-) or 3D printed PLA and PETG cut with cutting fluid (PLA+ (3D) and PETG+ (3D)). The smoothest and the roughest surface profiles are shown in figure 3 and figure 4 respectively.

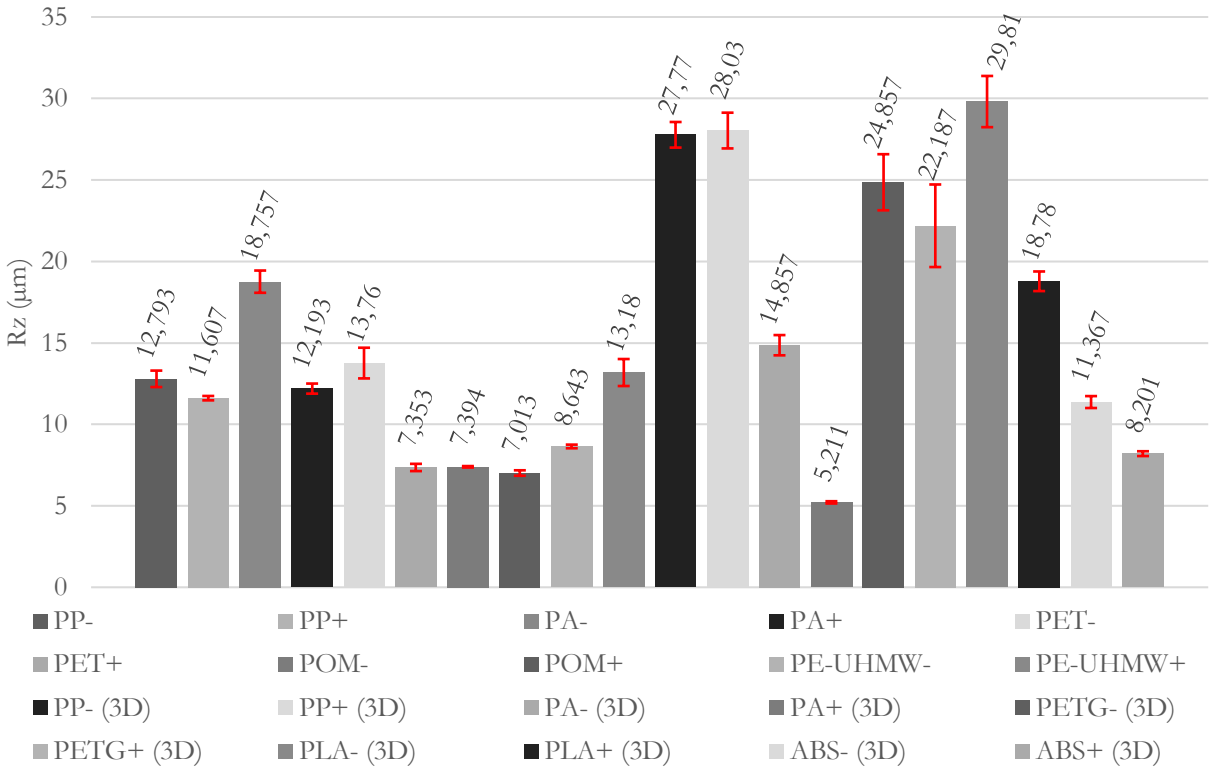

Graph 3 *Maximum average surface roughness Rz of evaluated surfaces*

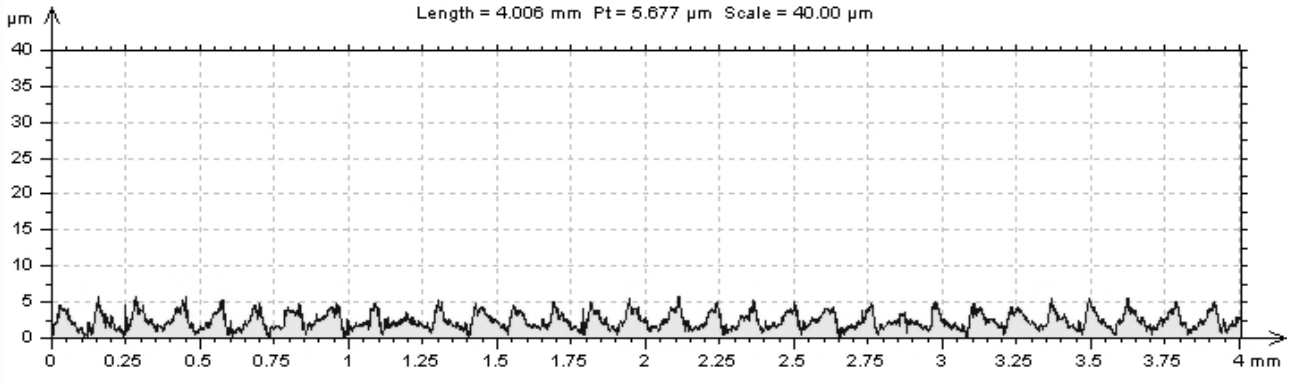

Fig. 3 *The achieved surface roughness on specimen PA+ (3D)*

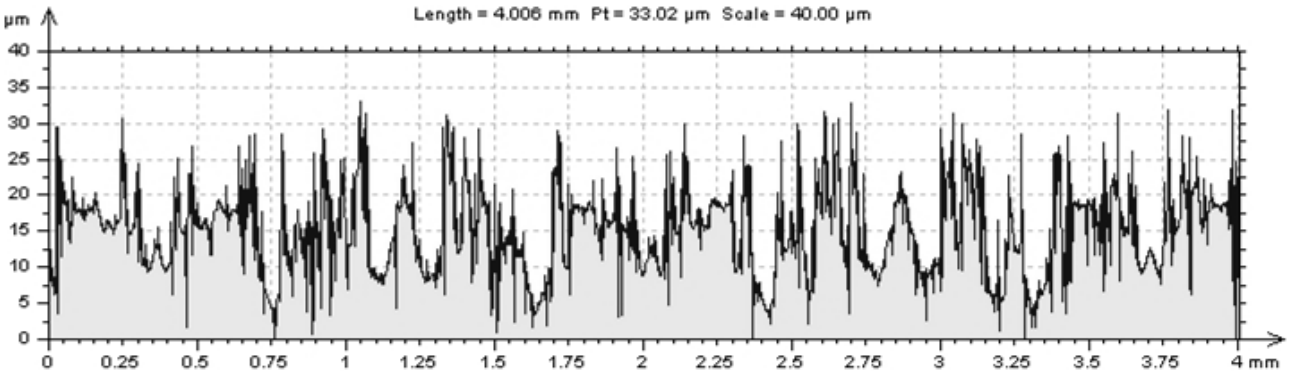

Fig. 4 *The measured surface roughness on specimen PP+ (3D)*

3D surface texture roughness Sa and Sz were measured with similar outcomes as presented in graphs 4 and 5 respectively, again showing PA+ (3D) being the best and PP+ (3D), PP- (3D) and PLA- (3D) being the worst. On PLA, the achieved surface roughness was also in agreement with what was measured by Martín-Bejár et al. [28] when turning PLA on a lathe. In general, machining seems to improve the surface roughness compared to printing alone, as was also presented by [23] et al. on PLA and PETG and Lalegani Dezaki et al. [25] on PETG.

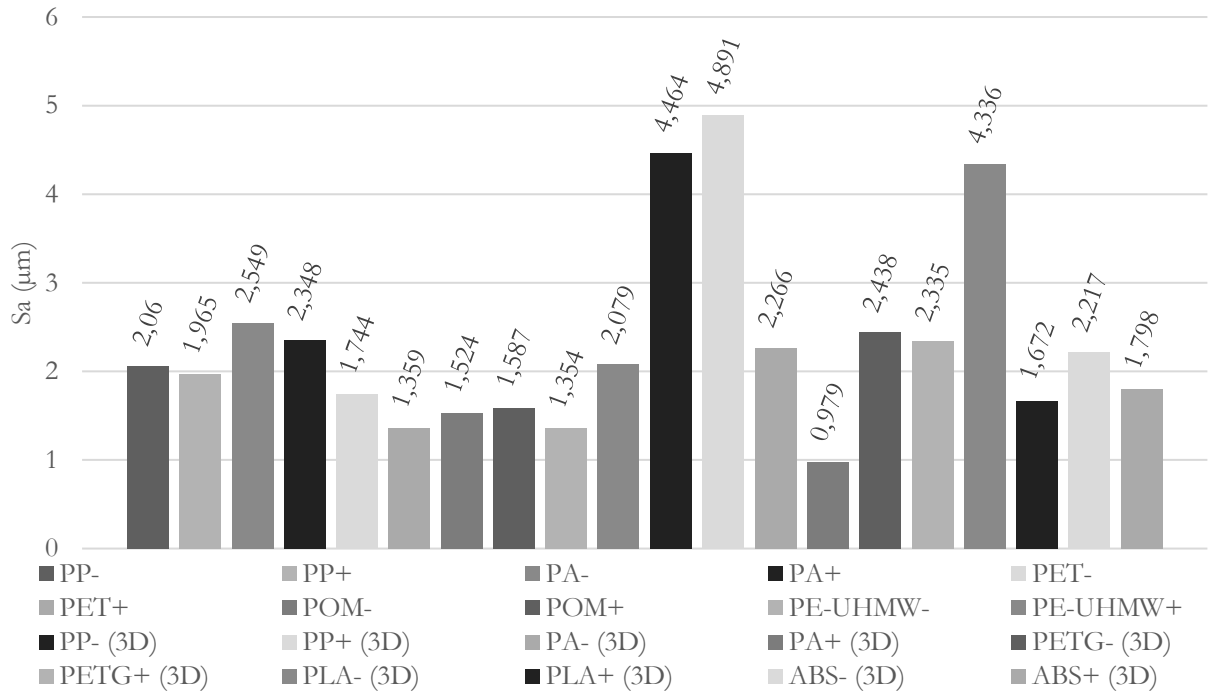

Graph 4 *Average texture height Sa of evaluated surfaces*

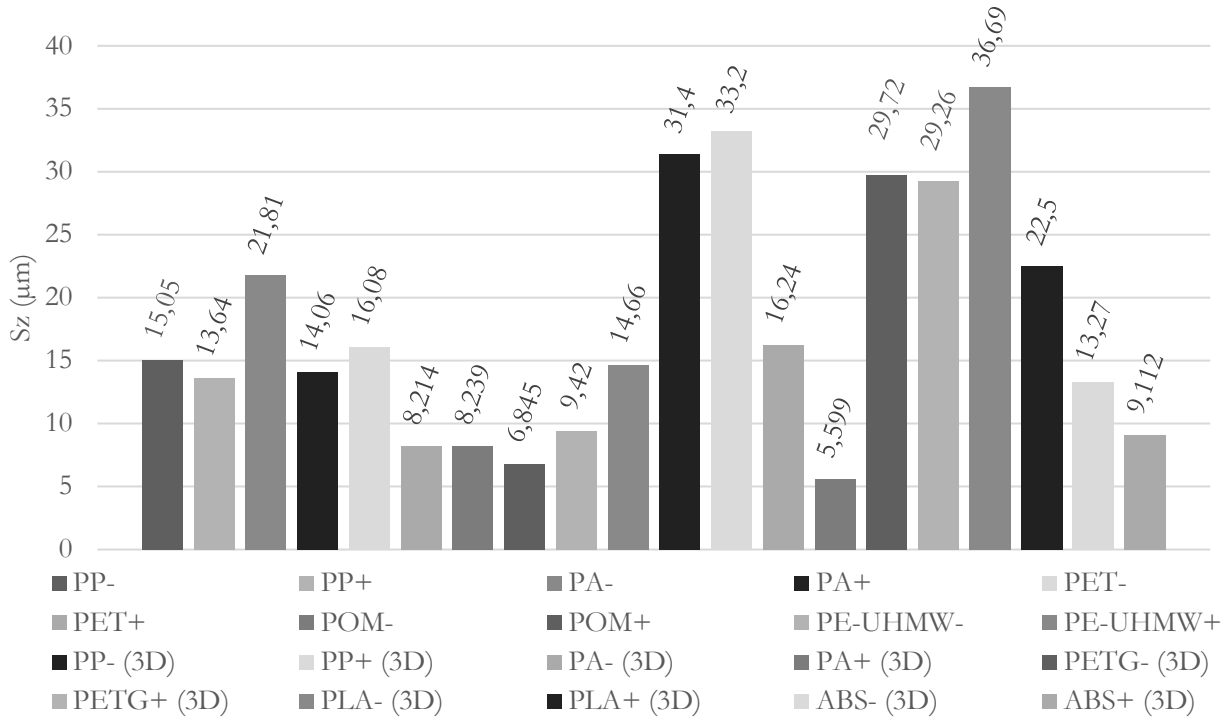

Graph 5 *Maximum average texture height Sz of evaluated surfaces*

PETG proved to be the best material in regard to its dimensional and geometric accuracy, but it is important to keep in mind that these values are more a result of the skills of the machinist and condition of the machine and clamping. Generally, extruded materials were able to achieve better surface quality than 3D printed ones, but best surface quality was achieved with 3D printed PA, cut with cutting fluid. The use of cutting fluid is recommended as it almost always improved the finish of the machined surface.

4 Conclusion

In this paper, two geometric parameters were assessed: dimensional accuracy of distance and parallelism. The smallest deviation in distance was recorded on a specimen made from polypropylene by extrusion. Other two highly accurate specimens were made from polyamide (PA) and polyethylene terephthalate glycol (PETG), both FDM 3D printed. This is a very important result, as PETG is one of the most commonly used materials for FDM printing. The highest deviation from nominal distance was found on the PET specimen. In comparison to the others, the value was so high that it was likely caused by an error during manufacturing. It is suspected to have been improperly clamped in the vise. When it comes to measuring parallelism, the best performing material was PETG made by 3D printing. Combined with its excellent dimensional accuracy, it is highly suitable for printing parts that will then be milled. On the other hand, the worst accuracy was recorded on the specimen, that was 3D printed from polypropylene.

When evaluating the surface quality, a total of 4 parameters were measured. On the 10 specimens, 20 surfaces were evaluated in total, as on each, one surface was cut dry and the other with cutting fluid. The parameters were divided into 2D profile roughness parameters and those related to 3D surface texture. According to the data on record, the lowest values of surface irregularities were measured on the surface that was machined using cutting fluid on the specimen made by 3D printing form polyamide (PA). On this surface, the lowest values were recorded on most of the evaluated parameters. The highest roughness values were measured on both surfaces on the 3D printed polypropylene specimen and on the dry cut surface on the part made from polylactic acid (PLA). The results of the surface quality assessment vary by a large margin, so choosing the right material for the application is crucial.

All things considered, the best combination of dimensional and geometric accuracy together with the smoothest machined surface was achieved with 3D printed polyamide machined with cutting fluid. It can thus be said that this material is most suited for milling post FDM 3D printing. It is also notable that using cutting fluid improved the achieved surface quality in 80% of cases.

Declaration of competing interest

The authors declare that they have no known competing financial interests or personal relationships that could have appeared to influence the work reported in this paper.

Data availability

Data will be made available on request.

Acknowledgment

This research study was supported by the grant "Comprehensive technology for interdisciplinary work with advanced materials, emphasizing their multidisciplinary applications" No.: FSI-S-25-8787.

References

[1] SEDLAK, J., JOSKA, Z., JANSKY, J., ZOUHAR, J., KOLOMY, S. et al. (2023). Analysis of the Mechanical Properties of 3D-Printed Plastic Samples Subjected to Selected Degradation Effects. In: *Materials,* Vol. 16, No. 8, pp. 3268. ISSN 1996-1944. https://doi.org/10.3390/ma16083268

[2] GEBHARDT, A., HÖTTER, J.-S. *Additive manufacturing: 3D printing for prototyping and manufacturing*. (2016). Cincinnati: Hanser Publications. ISBN 978-1-56990-582-1.

[3] KOLOMY, S., SLANY, M., DOUBRAVA, M., SEDLAK, J., ZOUHAR, J. et al. (2025). Comparative analysis of machinability and microstructure in LPBF and conventionally processed M300 maraging steel. In: *Scientific Reports*, Vol. 15, No. 1. ISSN 2045-2322. https://doi.org/10.1038/s41598-025-19719-8

[4] KOLOMY, S., MALY, M., DOUBRAVA, M., SEDLAK, J., ZOUHAR, J. et al. (2025) Effect of microstructure on machinability of extruded and conventional H13 tool steel. In: *Materials & design*, Vol. 254, pp. 114132. ISSN 0264-1275. https://doi.org/10.1016/j.matdes.2025.114132

[5] KOLOMY, S., BENC, M., HARANT, M., SEDLAK, J., JOPEK, M. (2024) Effect of different strain rates on mechanical behavior and structure of Inconel 718 produced by powder bed fusion. In: *International Journal of Mechanics and Materials in Design*, Vol. 21, No. 1, pp. 1-16. ISSN 1569-1713. https://doi.org/10.1007/s10999-024-09724-6

[6] *What is SLA printing? The original resin 3D print method.* (2025). In: Protolabs Network. https://www.hubs.com/knowledge-base/what-is-sla-3d-printing/

[7] CHUA, CH., LEONG, K. F. (2017). *3D printing and additive manufacturing: principles and applications*. Fifth edition of Rapid prototyping. New Jersey: World Scientific. ISBN 978-981-3146-76-1.

[8] DE NAOUM, K. (2022). *SLS vs. SLM: Here's What You Should Know About These Printing Methods*. In: Xometry. https://www.xometry.com/resources/3d-printing/sls-vs-slm-3d-printing/

[9] *FDM vs. SLA 3D printing*. (2025) In: Protolabs Network. https://www.hubs.com/knowledge-base/fdm-vs-sla-3d-printing/

[10] LAY, M., THAJUDIN, N. L. N., HAMID, Z. A. A., RUSLI, A., ABDULLAH, M. K. et al. (2019). Comparison of physical and mechanical properties of PLA, ABS and nylon 6 fabricated using fused deposition modeling and injection molding. In: *Composites Part B: Engineering*, Vol. 176, pp. 107341. ISSN 1359-8368. https://doi.org/10.1016/j.compositesb.2019.107341

[11] CHACÓN, J.M., CAMINERO, M.A., GARCÍA-PLAZA, E., NÚÑEZ, P.J. (2017). Additive manufacturing of PLA structures using fused deposition modelling: Effect of process parameters on mechanical properties and their optimal selection: Effect of process parameters on mechanical properties and their optimal selection. In: *Materials & Design*, Vol. 124, pp. 143-157. ISSN 0264-1275. https://doi.org/10.1016/j.matdes.2017.03.065

[12] SHAFFER, S., YANG, K., VARGAS, J., DI PRIMA, M. A., VOIT, W. (2014). On reducing anisotropy in 3D printed polymers via ionizing radiation. In: *Polymer*, Vol. 55, No. 23, pp. 5969-5979. ISSN 0032-3861. https://doi.org/10.1016/j.polymer.2014.07.054

[13] WITTBRODT, B., PEARCE, J., M. (2015). The effects of PLA color on material properties of 3-D printed components. In: *Additive Manufacturing*, Vol. 8, pp. 110-116. ISSN 2214-8604. https://doi.org/10.1016/j.addma.2015.09.006

[14] KUZNETSOV, V., SOLONIN, A., URZHUMTSEV, O., CHILLING, R., TAVITOV, A. (2018). Strength of PLA Components Fabricated with Fused Deposition Technology Using a Desktop 3D Printer as a Function of Geometrical Parameters of the Process. In: *Polymers*, Vol. 10, No. 3, pp. 313. ISSN 2073-4360. https://doi.org/10.3390/polym10030313

[15] İNCESU, R., AKDERYA, T. (2024). The Influence of Printing Speed and Temperature on the Mechanical, Absorptive, and Morphological Properties of PLA-Based Hybrid Materials Produced with an FDM-Type 3D Printer. In: *Polymers*, Vol. 16, No. 19, pp. 2771. ISSN 2073-

4360. https://doi.org/10.3390/polym16192771

[16] HSUEH, M. H., LAI, CH. J., WANG, S.-H., ZENG, Y.-S., HSIEH, CH.-H. et al. (2021). Effect of Printing Parameters on the Thermal and Mechanical Properties of 3D-Printed PLA and PETG, Using Fused Deposition Modeling. In: *Polymers*, Vol. 13, No. 11, pp. 1758. ISSN 2073-4360. https://doi.org/10.3390/polym13111758

[17] RODRÍGUEZ-PANES, A., CLAVER, J., CAMACHO, A. M. (2018). The Influence of Manufacturing Parameters on the Mechanical Behaviour of PLA and ABS Pieces Manufactured by FDM: A Comparative Analysis: A Comparative Analysis. In: *Materials*, Vol. 11, No. 8, pp. 1333. ISSN 1996-1944. https://doi.org/10.3390/ma11081333

[18] [18] VINYAS, M., ATHUL, S.J., HARURSAMPATH, D., NGUYEN THOI, T. (2019). Mechanical characterization of the Poly lactic acid (PLA) composites prepared through the Fused Deposition Modelling process. In: *Materials Research Express*, Vol. 6, No. 10, pp. 105359. ISSN 2053-1591. https://doi.org/10.1088/2053-1591/ab3ff3

[19] TORRADO, A. R., SHEMELYA, C. M., ENGLISH, J. D., LIN, Y., WICKER, R. B. et al. (2015). Characterizing the effect of additives to ABS on the mechanical property anisotropy of specimens fabricated by material extrusion 3D printing. In: *Additive Manufacturing*, Vol. 6, pp. 16-29. ISSN 2214-8604. https://doi.org/10.1016/j.addma.2015.02.001

[20] AGRAWAL, A. P., KUMAR, V., KUMAR, J., PARAMASIVAM, P., DHANASEKARAN, S. et al. (2023). An investigation of combined effect of infill pattern, density, and layer thickness on mechanical properties of 3D printed ABS by fused filament fabrication. In: *Heliyon*, Vol. 9, No. 6, pp. 16531. ISSN 2405-8440. https://doi.org/10.1016/j.heliyon.2023.e16531

[21] ALAUDDIN, M., CHOUDHURY, I.A., EL BARADIE, M.A., HASHMI, M.S.J. (1995). Plastics and their machining: A review: A review. In: *Journal of Materials Processing Technology*, Vol. 54, No. 1-4, pp. 40-46. ISSN 0924-0136. https://doi.org/10.1016/0924-0136(95)01917-0

[22] TEZEL, T. (2021). The effect of machining parameters on the surface quality of 3D printed and cast polyamide. In: *Machining Science and Technology*, Vol. 25, No. 5, pp. 703-720. ISSN 1091-0344. https://doi.org/10.1080/10910344.2021.1971704

[23] MEHTEDI, M. E., BUONADONNA, P., MOHTADI, R. E., AYMERICH, F., CARTA, M. (2024). Surface quality related to machining parameters in 3D-printed PETG components. In: *Procedia Computer Science*, Vol. 232, pp. 1212-1221. ISSN 1877-0509. https://doi.org/10.1016/j.procs.2024.01.119

[24] PĂMĂRAC, R. G., PETRUSE, R. E. (2018). Study Regarding the Optimal Milling Parameters for Finishing 3D Printed Parts from ABS and PLA Materials. In: *ACTA Universitatis Cibiniensis*, Vol. 70, No. 1, pp. 66-72. ISSN 1583-7149. https://doi.org/10.2478/aucts-2018-0009

[25] LALEGANI DEZAKI, M., MOHD ARIFFIN, M. K. A., ISMAIL, M. I. S. (2020). Effects of CNC Machining on Surface Roughness in Fused Deposition Modelling (FDM) Products. In: *Materials*, Vol. 13, No. 11, pp. 2608. ISSN 1996-1944. https://doi.org/10.3390/ma13112608

[26] ÇEVIK, Z. A. (2025). The Effect of FDM Process Parameters on the Machinability of Pet-G Material: Delamination Analysis Using the Taguchi Approach. In: *International Journal of 3D Printing Technologies and Digital Industry*, Vol. 9, No. 2, pp. 310-319. ISSN 2602-3350. https://doi.org/10.46519/ij3dptdi.1704399

[27] SHUNMUGESH, K., GANESH, M., BHAVANI, R., KHAN, M. A., SARAVANA KUMAR, M. et al. (2025). Enhancing drilling performance in 3D printed PLA implants application of PIV and ML models. In: *Scientific Reports*, Vol. 15, No. 1. ISSN 2045-2322. https://doi.org/10.1038/s41598-025-96126-z

[28] MARTÍN-BÉJAR, S., BAÑÓN-GARCÍA, F., BERMUDO GAMBOA, C., SEVILLA HURTADO, L. (2025). Machinability and Geometric Evaluation of FFF-Printed PLA-Carbon Fiber Composites in CNC Turning Operations. In: *Applied Sciences*, Vol. 15, No. 15, pp. 8141. ISSN 2076-3417. https://doi.org/10.3390/app15158141

[29] KHAIRUSSHIMA, M.K.N., AMIN, A.K.M., CHE HASSAN, C.H., JAHARAH, A.G. (2015). Tool Wear during Milling Laminated Carbon Fibre Reinforced Plastic. In: *Advanced Materials Research*, Vol. 1115, pp. 96-99. ISSN 1662-8985. https://doi.org/10.4028/www.scientific.net/AMR.1115.96

[30] SEDLAK, J., ZOUHAR, J., KOLOMY, S., SLANY, M., NECESANEK, E. (2023). Effect of high-speed steel screw drill geometry on cutting performance when machining austenitic stainless steel. In: *Scientific reports*, Vol. 13, No. 1, pp. 9233-9233. ISSN 2045-2322. https://doi.org/10.1038/s41598-023-36448-y

[31] DRBAL, M., KOLOMY, S., SEDLAK, J., ZOUHAR, J., VITEK, J. (2024). Investigation of the Tool Wear Progression in Parting Technology. In: *Manufacturing Technology*, Vol. 24, No. 6, pp. 901-913. ISSN 1213-2489. https://doi.org/10.21062/mft.2024.093

[32] MALY, M., KOLOMY, S., KASAN, R., BARTL, L., SEDLAK, J. et al. (2024). Mechanical Properties, Structure and Machinability of the H13 Tool Steel Produced by Material Extrusion. In: *Manufacturing Technology*, Vol. 24, No. 4, pp. 608-617. ISSN 1213-2489. https://doi.org/10.21062/mft.2024.066

[33] ZEMČÍK, O., KOUŘIL, K., SLANÝ, M., ZOUHAR, J., SEDLÁK, J. et al. (2023). Machinability of UMCo50 Cobalt Superalloy. In: *Manufacturing Technology*, Vol. 23, No. 6, pp. 949-957. ISSN 1213-2489. https://doi.org/10.21062/mft.2023.082